Perilobar Nephrogenic Rests Are Nonobligate Molecular Genetic Precursor Lesions of Insulin-Like Growth Factor-II-Associated Wilms Tumors

Raisa Vuononvirta,[1] Neil J. Sebire,[2] Anthony R. Dallosso,[5] Jorge S. Reis-Filho,[3] Richard D. Williams,[1] Alan Mackay,[3] Kerry Fenwick,[3] Anita Grigoriadis,[3,4] Alan Ashworth,[3] Kathy Pritchard-Jones,[1] Keith W. Brown,[5] Gordan M. Vujanic,[6] and Chris Jones[1]

Abstract

Purpose: Perilobar nephrogenic rests (PLNRs) are abnormally persistent foci of embryonal immature blastema that have been associated with dysregulation at the 11p15 locus by genetic/epigenetic means and are thought to be precursor lesions of Wilms tumor. The precise genomic events are, however, largely unknown.

Experimental Design: We used array comparative genomic hybridization to analyze a series of 50 PLNRs and 25 corresponding Wilms tumors characterized for 11p15 genetic/epigenetic alterations and insulin-like growth factor-II expression.

Results: The genomic profiles of PLNRs could be subdivided into three categories: those with no copy number changes (22 of 50, 44%); those with single, whole chromosome alterations (8 of 50, 16%); and those with multiple gains/losses (20 of 50, 40%). The most frequent aberrations included 1p- (7 of 50, 14%) +18 (6 of 50, 12%), +13 (5 of 50, 10%), and +12 (3 of 50, 6%). For the majority (19 of 25, 76%) of cases, the rest harbored a subset of the copy number changes in the associated Wilms tumor. We identified a temporal order of genomic changes, which occur during the insulin-like growth factor-II/PLNR pathway of Wilms tumorigenesis, with large-scale chromosomal alterations such as 1p-, +12, +13, and +18 regarded as "early" events. In some of the cases (24%), the PLNRs harbored large-scale copy number changes not observed in the concurrent Wilms tumor, including +10p, +14q, and +18.

Conclusions: These data suggest that although the evidence for PLNRs as precursors is compelling, not all lesions must necessarily undergo malignant transformation.

The cell of origin of Wilms tumor (nephroblastoma) is thought to be the metanephric blastemal cell, which forms a pluripotent renal stem cell population during organogenesis and, in response to penetration by the ureteric bud, induces branching morphogenesis and subsequent kidney development (1, 2). In a paradigm of the links between abrogated organ development and tumorigenesis, these pluripotent cells may persist beyond 36 weeks of gestation and appear in up to 1% of routine infant postmortem as nephrogenic rests (3). These lesions are thought to be precursors of Wilms tumors, as they are reported to be found in 30% to 40% of kidneys containing a sporadic tumor and in close to 100% of bilateral cases (3). Their natural history is, however, uncertain: most appear to spontaneously involute, as they are rarely observed in normal kidneys after age 1 year (3).

Nephrogenic rests are histologically classified as either perilobar (PLNR) or intralobar (ILNR), and both types may be further described as dormant, sclerosing, adenomatous, or hyperplastic (3). PLNRs are usually multifocal, are found at the periphery of the renal lobe, are sharply demarcated, and usually consist of blastema and tubules (3). In contrast, ILNRs are often unifocal, are randomly situated within the renal lobe, show poorly defined, irregular, and intermixed margins, and are more commonly composed of stroma (usually predominant), blastema, and tubules (3). Clues to the genetic components of their persistence come from their links to developmental syndromes: PLNRs are associated with overgrowth syndromes including hemihypertrophy and Beckwith-Wiedemann-syndrome, whereas ILNRs are commonly found in WAGR (Wilms tumor-aniridia-genital anomaly-mental retardation) and Denys-Drash syndromes (4).

Direct evidence for the genetic link of rests to Wilms tumor evolution is limited but compelling. Most striking is the

Authors' Affiliations: [1]Paediatric Oncology, Institute of Cancer Research/Royal Marsden NHS Trust, Sutton, United Kingdom; [2]Department of Histopathology, Great Ormond Street Hospital for Children; [3]Breakthrough Breast Cancer Research Centre, Institute of Cancer Research; [4]Ludwig Institute for Cancer Research, London, United Kingdom; [5]Department of Cellular and Molecular Medicine, University of Bristol, Bristol, United Kingdom; and [6]Department of Pathology, University of Wales College of Medicine, Cardiff, United Kingdom

Received 6/24/08; revised 7/23/08; accepted 8/2/08.

Grant support: Cancer Research UK, Breakthrough Breast Cancer, CLIC Sargent, and University of Bristol Cancer Research Fund.

The costs of publication of this article were defrayed in part by the payment of page charges. This article must therefore be hereby marked *advertisement* in accordance with 18 U.S.C. Section 1734 solely to indicate this fact.

Requests for reprints: Chris Jones, Paediatric Oncology, Institute of Cancer Research/Royal Marsden NHS Trust, 15 Cotswold Road, Sutton, Surrey SM2 5NG, United Kingdom. Phone: 44-20-8722-4416; Fax: 44-20-8722-4321; E-mail: chris.jones@icr.ac.uk.

doi:10.1158/1078-0432.CCR-08-1620

Translational Relevance

The presence of nephrogenic rests in a child's kidney has been considered to confer an increased risk of Wilms tumor. Here, we report the molecular genetic basis of the precursor status of these lesions. By defining a temporal order of the genomic alterations occurring during Wilms tumor pathogenesis, we are able to identify those key changes associated with malignancy and distinguish them from "passenger" alterations. This has implications for the diagnostic dilemmas of differential diagnosis between nephrogenic rest and overt Wilms tumor and has translational relevance for treatment guidance in the clinic.

identification of heterozygous mutations of the *WT1* gene in PLNRs and homozygous mutations in a few hyperplastic ILNRs (5), although this has not been explored further. In an allelic imbalance study, Charles et al. observed a more frequent loss of heterozygosity (LOH) at 11p13 (*WT1* locus) in ILNRs, with a stronger association of alterations at 11p15 (*WT2* locus) with PLNRs (6). It is notable that the LOH on chromosome 11p preferentially involves the maternal chromosome and results in a uniparental disomy of the paternal allele and biallelic insulin-like growth factor-II (IGF-II) expression (7). These cases with LOH harbored the same abnormalities in the adjacent Wilms tumor, suggesting that aberrations at *WT1*/*WT2* in nephrogenic rests may represent early genetic events in Wilms tumorigenesis.

The occurrence of epigenetic events on chromosome 11p provides the best studied lines of evidence. Loss of imprinting (LOI) at the *WT2* locus on 11p15 is found in 33% to 50% of Wilms tumors (4), shows a marked ethnic variation (8), and has been observed in PLNRs (9). Aberrant imprinting control at this locus appears restricted to the genes *IGF-II* and *H19* (10), with hypermethylation of the *H19* differentially methylated region on the maternal allele preventing binding of the CTCF chromatin insulator, resulting in *IGF-II* LOI and biallelic expression. It has been suggested that sporadic Wilms tumor with *IGF-II* LOI is part of a spectrum of prenatal and postnatal overgrowth disorders associated with epigenetic mosaicism at the *IGF-II* locus (8) and that PLNRs are a morphologic consequence of the renal *IGF-II* mosaicism (9).

The Wilms tumors themselves, which are thought to arise from PLNRs or ILNRs, appear to have distinct morphologic features. "ILNR-like" tumors tend to show a spectrum of mesenchymal differentiation with the stromal-predominant histology associated with the underlying genetics (*WT1*/*β-catenin* mutation; ref. 11). By contrast, the "PLNR-like" tumors tend to show a limited nephrogenic differentiation with a marked blastemal and, to a lesser extent, epithelial cell predominance (12). These tumors harbor either LOH and subsequent uniparental disomy or LOI of the *IGF-II*/*H19* locus resulting in a marked overexpression of IGF-II in the tumor cells. Coupled with our recent identification of blastemal cell copy number gain and overexpression of the *IGF-I receptor* in chemoresistant Wilms tumors (13), these tumors may be considered to be driven by IGF signaling in an autocrine/paracrine fashion.

We have investigated the genomic events associated with the earliest stages of the development of these IGF-II-associated Wilms tumors by examining a series of sporadic PLNRs, characterized for genetic and epigenetic aberrations at 11p15, by applied array comparative genomic hybridization (aCGH), and provide the first genomic evidence of the nonobligate precursor role of PLNRs in Wilms tumorigenesis.

Materials and Methods

Samples and DNA extraction. Archival pathology specimens of PLNRs and corresponding Wilms tumors from the same patients were obtained from the Royal Marsden and Great Ormond Street Hospitals with full ethical committee approval. All cases were reviewed by three pathologists (N.J.S., G.M.V., and J.S.R-F.). In total, 50 formalin-fixed, paraffin-embedded (FFPE) PLNRs were obtained from 42 nonsyndromic patients, with matched Wilms tumors from 25 cases. The vast majority (46 of 50, 92%) exhibited a high degree of WT1 protein expression by immunohistochemistry. There was an overrepresentation of patients with bilateral disease (17 of 50, 34%), as rests are known to be more prevalent in these cases. Lesions were subjected to either laser capture microdissection (PixCell LCM System; Arcturus) or manual microdissection according to the relative size and location of the rests. The vast majority of cases were treated with preoperative chemotherapy, which we have shown previously not to harbor significant genomic differences to those taken at immediate nephrectomy (14). Sections were stained with nuclear fast red to aid in morphologic assessment without interfering with downstream amplification protocols. The DNeasy Tissue Kit (Qiagen) was used for DNA extraction according to the manufacturer's protocol. For the laser-captured samples, up to three subsequent rounds of additional proteinase K digestions at 55°C overnight were carried out. DNA quantitation was determined by spectrophotometry (NanoDrop). We have reported previously the GenomePlex whole-genome amplification technique to be a highly accurate and reproducible method to amplify DNA samples from FFPE material for aCGH analysis using as little as 5 ng starting DNA (15). For the whole-genome amplification of the microscopic, laser-captured nephrogenic rests (up to 3,000 cells), an improved version of the kit ("WGA4"; Sigma) was used according to the manufacturer's protocol.

aCGH. All raw and processed data have been deposited in Array Express[7] (E-TABM-436). The aCGH platforms used in this study were constructed at the Breakthrough Breast Cancer Research Centre. Hybridizations were carried out as described previously (14) onto a 5.8K, 0.9 Mb-spaced (E-MEXP-213) and/or a 16K, 100 kb-spaced (E-MEXP-1040) BAC array. Slides were scanned using an Axon 4000B scanner (Axon Instruments) and images were analyzed using Genepix Pro 4.1 software (Axon Instruments). The median localized background slide signal for each clone was subtracted and each clone Cy5/Cy3 ratio normalized by local regression (loess) against fluorescence intensity, print-tip subarray, and within-block spatial location. Data were further scaled by dividing each clone by its median absolute deviation. BAC clone replicate spots were averaged, and clones with poor reproducibility between replicates were excluded (SD > 0.2). In addition, clones with missing/poor values in >70% samples were also excluded as were those with no mapping information (March 2006 build of the human genome sequence, hg18). To allow integration of the two platforms, the 16K-derived data were reduced to the resolution of the 5.8K platform by taking the median value of the nearest clones within 1 Mb of the corresponding lower-resolution landmark. In this way, we were left with a final data set comprising 75 samples with 3,342 data points each.

[7] www.ebi.ac.uk/arrayexpress/

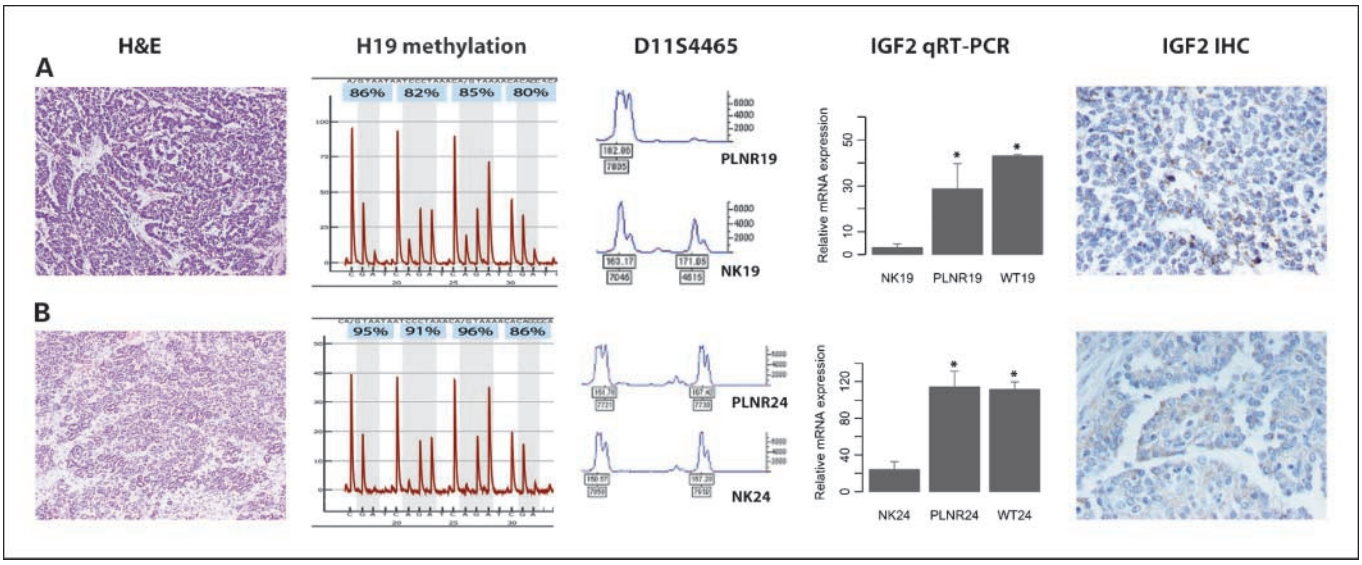

Fig. 1. Genetic and epigenetic means of IGF-II overexpression in PLNRs. *A,* LOH at 11p15 in a hyperplastic PLNR19 (H&E, ×100) as seen by H19 methylation and allelic imbalance. In addition, there is increased IGF-II mRNA (RT-PCR) and protein (immunohistochemistry, ×400). *B,* LOI at 11p15 in a sclerosing/regressive/adenomatous PLNR24 (H&E, ×100) as seen by high levels of H19 methylation and the absence of allelic balance. There is also increased IGF-II mRNA (RT-PCR) and protein (immunohistochemistry, ×400). Hypermethylation (*blue boxes*) at CpG islands (*shaded*) at the *H19* differentially methylated region was assessed by pyrosequencing of the reverse strand. Polymorphic probe D11S4465 showing one or two peaks on an ABI7700 Genetic Analyzer. *NK,* normal kidney from same patient as PLNR. *, $P < 0.05$, *t* test.

Statistical analysis. All data transformation and statistical analysis were carried out in R 2.0.1[8] and Bioconductor 1.5,[9] making extensive use of modified versions of the package aCGH in particular (14). For identification of DNA copy number alterations, data were smoothed using a local polynomial adaptive weights procedure for regression problems with additive errors, with thresholds for assigning "gain" and "loss" derived from the overall median absolute deviation of each sample. For visualization purposes, the processed $\log_2$ ratios were colored green (gain) or red (loss) after segmentation and copy number determination. Thresholded data for each clone were used for categorical analysis using a Fisher's exact test and paired statistics in significance analysis of microarrays, with a correction for multiple testing using the step-down permutation procedure maxT, providing strong control of the family-wise type I error rate.

The copy number data set was converted to wiggle track (WIG) format by a custom Perl script and displayed on the University of California-Santa Cruz genome browser[10] in parallel with the positions of known copy number variations in the HapMap populations (16). Copy number changes in the current data that overlapped with these copy number variations were excluded from further analysis.

Statistical analysis of categorical data between different subgroups was carried out by Fisher's exact test and between continuous variables using the Mann-Whitney *U* test. $P < 0.05$ was considered significant. Concordance and similarity scores were calculated as described previously (17). Briefly, the percent concordance equates to the number of changes in common between a pair of samples divided by the number in common plus half the sum of the number of changes in only one or other of the pair. The similarity score was calculated as a weighted sum of all observed alterations based on the frequency of the changes in a larger Wilms tumor population (14). Such similarity scores will be increasingly positive when pairs are more alike.

Methylation analysis of the H19 differentially methylated region. Genomic DNA (300 ng) was bisulfite converted using the EZ DNA Methylation-Gold kit (Zymo Research) according to the manufacturer's instructions. Converted DNA was amplified by PCR using JumpStart REDTaq DNA polymerase (Sigma-Aldrich) for 45 cycles with H19pyroF 5′-GATTTTGATGGGGTTAGGATGT and H19pyroR 3′-CTCCTACTC-CAAACATTATAAAA oligonucleotide primers (Eurogentec). Pyrosequencing was carried out using the PyroGold SQA reagent kit (Pyrosequencing AB) according to the manufacturer's instructions with the sequencing primer H19pyroS 5′-TATAAACAAATTCACCTCTC.

Loss of heterozygosity. LOH analysis was done as described previously (18), with the forward primer labeled fluorescently with either tetrachlorofluorescein or hexachlorofluorescein dyes (Invitrogen). Sequences of primers for markers at 11p15 were as follows: D11S4465 forward TAGCCCAAATATCATGTGCA and reverse TGACTGTCACTTAGTAGATGCTCC and TH forward CCTCCCCAGG-GCGGCCCGGGGCCCA and reverse CACTTACTTACCCTTGG-GGTGGGGG. PLNR, Wilms tumor, and corresponding normal DNA were amplified using touchdown 68-50 program for 35 cycles as follows: denaturing at 94°C for 10 min followed by 95°C for 30 s, 68°C for 45 s, decreasing by 1°C with every cycle followed by incubation at 72°C for 1 min for 17 more times. This was then followed by 94°C for 30 s, 50°C for 45 s, and 72°C 1 min and repeated for 34 more times, with a subsequent final extension at 72°C for 5 min. Each PCR was done under standard conditions in a 15 μL reaction volume containing 250 ng template DNA, 0.8 μmol/L of each primer, 0.2 μmol/L deoxynucleotide triphosphate, 1.5 mmol/L $MgCl_2$, 0.2 units Taq polymerase (ABGene), and 1× PCR buffer. Denatured reaction products were analyzed on an ABI 7700 capillary sequencer (Applied Biosystems) and visualized with Genotyper software (Applied Biosystems). Allele ratios for PLNR or Wilms tumor compared with normal DNA were calculated as (A1/A2)T/(A1/A2)N and LOH was scored if this ratio was <0.5 and >2.0 in one or both markers.

Quantitative reverse transcription-PCR. RNA extraction for all FFPE samples was carried out by using RNeasy FFPE kit (Qiagen) according to the manufacturer's instructions. cDNA was prepared from 10 μg RNA by random primed reverse transcription using a High-Capacity cDNA Reverse Transcription kit from Applied Biosystems. IGF-II Assay-on-Demand (Hs00171254_m1) was obtained from Applied Biosystems. PCRs were done in a 10 μL reaction volume containing 5 μL of 2× buffer/enzyme mix, 1 μL of 20× assay mix, 1 μL of 20× GAPDH (4326317E), or HPRT1 (4326321E) endogenous control assay mix and

[8] http://www.r-project.org/
[9] http://www.bioconductor.org/
[10] http://genome.ucsc.edu

Table 1. Summary of genetic and epigenetic alterations in PLNRs and associated Wilms tumors

Case	PLNR	Histology	WT1	Ki-67	LOI 11p15	LOH 11p15	RT-PCR	Immunohisto-chemistry IGF-II	PLNR aCGH
1	1	Sclerosing/hyperplastic	-	3	NA	NA	NA	+	None
2	2	Nephroblastomatosis	+	12	LOI	-	+	+	None
3	3	Hyperplastic	+	4	meth	LOH	NA	+	-1p36
4	4	Hyperplastic	+	2	LOI	-	-	+	None
5	5	Obsolescent	-	0	-	-	-	+	None
6	6	Hyperplastic	-	31	meth	LOH	+	+	None
7	7	Sclerosing	+	1	NA	-	-	+	+10p15, +13, +14, +18
8	8	Sclerosing/adenomatous	+	10	meth	LOH	-	+	-1p36, +12, -19
9	9	Regressive	+	1	NA	-	-	+	-21q
10	10	Sclerosing	+	1	meth	NA	+	+	None
11	11	Hyperplastic	+	3	LOI	-	-	-	None
12	12	Regressing/adenomatous	+	2	NA	LOH	NA	+	+10p15, -11q, +14, +18
13	13	Dormant	+	5	LOI	-	+	+	-7p, +7q11-q21, -7q22-q35, -11p13
14	14	Sclerosing/regressive	+	5	-	-	NA	-	+10p15, +13, +14, +18
15	15	Sclerosing	+	33	LOI	-	+	-	+12, +17, +18
16	16	Sclerosing	+	1	LOI	-	+	+	-1p36
17	17	Regressive	+	2	LOI	-	+	-	None
18	18	Hyperplastic	+	2	LOI	-	+	+	None
19	19	Hyperplastic	+	70	meth	LOH	+	+	+6, +7, -18q, +22q
20	20	Sclerosing	+	13	LOI	-	+	+	-1p36, +12, +18
21	21	Sclerosing/adenomatous	+	4	LOI	-	+	+	-1p36, -7p, +7q21, -12q24, -19
22	22	Sclerosing	+	6	LOI	-	+	-	+10p15, +13
23	23	Sclerosing	+	13	meth	LOH	+	+	None
24	24	Sclerosing/regressive/ adenomatous	+	3	LOI	-	+	+	-1p36, -22q
25	25	Sclerosing	+	1	LOI	-	-	+	-12q24, +18
26	26	Hyperplastic	+	3	NA	NA	-	+	None
27	27	Sclerosing	-	8	NA	-	+	-	-4p, +4q
28	28	Adenomatous	+	15	NA	-	-	+	+4p, +8q24, +11, -19q13
29	29	Hyperplastic	+	7	NA	-	+	-	None
30	30	Sclerosing	+	3	NA	-	+	+	None
31	31	Sclerosing/adenomatous	+	12	meth	NA	-	-	-1p36, +4, +5p, +13q, -22q
32	32	Sclerosing	+	4	-	NA	-	+	-11q13
33	33	Dormant	+	NA	NA	NA	NA	-	None
34	34	Sclerosing	+	1	LOI	-	-	+	None
35	35	Nephroblastomatosis	+	28	meth	NA	+	-	-9p, -11q, +15q26
36	36	Sclerosing	+	1	LOI	-	NA	+	None
37	37	Sclerosing/dormant	+	2	LOI	-	NA	+	None
38	38	Adenomatous/hyperplastic	+	6	meth	NA	+	NA	-11p
	39	Sclerosing	+	4	meth	NA	NA	+	+2p24, -11p
39	40	Sclerosing	+	5	LOI	-	NA	NA	-11p13
	41	Regressive/adenomatous	+	4	LOI	-	-	+	-4p, +4q, -11p, +11q, +13, +18q12, -20q
40	42	Regressive/hyperplastic	+	2	LOI	-	NA	-	None
	43	Regressive/hyperplastic	+	2	LOI	-	NA	-	-12q24
	44	Regressive/hyperplastic	+	3	LOI	-	NA	NA	+7, -18q21
41	45	Regressive	+	4	LOI	-	+	-	+X
	46	Hyperplastic	+	6	LOI	-	NA	NA	15q26, +X
42	47	Sclerosing	+	0	meth	LOH	+	+	None
	48	Hyperplastic	+	1	meth	LOH	NA	-	None
	49	Hyperplastic	+	1	meth	LOH	NA	NA	None
	50	Adenomatous	+	5	meth	LOH	NA	NA	None

NOTE: Listed are the cases profiled by aCGH and includes histology, 11p15 LOH, IGF-II LOI, IGF-II RT-PCR, IGF-II immunohistochemistry, Ki-67 (%) immunohistochemistry, and copy number changes by aCGH. Concordance and similarity scores between matched PLNRs and Wilms tumors are also given.
Abbreviations: meth, methylation of *H19;* LOI, LOI for IGF-II defined by *H19* hypermethylation in the absence of allelic imbalance; LOH, LOH at the 11p15 locus; +, expressed; -, negative; NA, not done, not informative, or not worked.

1 μL input cDNA. Assays were run on an Applied Biosystems 7900 Sequence Detection System and results were analyzed by the standard curve method. Data were normalized to Universal Human Reference RNA (Stratagene).

Immunohistochemistry. Immunohistochemistry was done on 5 μm FFPE sections using a mouse monoclonal antibody to either human Ki-67 clone MIB-1 (M7240; DAKO), WT1 clone 6FH2 (M3561 DAKO), or IGF-II (ab9574; Abcam) using the Envision horseradish peroxidase

Table 1. Summary of genetic and epigenetic alterations in PLNRs and associated Wilms tumors (Cont'd)

Wilms tumor	WT1	Ki-67	LOI 11p15	LOH 11p15	RT-PCR	Immunohisto-chemistry IGF-II	Wilms tumor aCGH	Concordance (%)	Similarity
1	+	12	NA	NA	NA	+	-17, +18	0	-6.05
2	+	14	LOI	-	+	+	+19	0	-4.62
3	+	14	-	LOH	NA	+	-1p36	100	3.74
4	+	63	meth	LOH	-	+	+4q, -10p, +13, -14q, -17p	0	-12.23
5	+	0	NA	-	+	+	-1p36, +1q, -2q37, +6, -7, +8, +12, +13	0	-17.21
6	+	15	LOI	-	+	-	-11p13	0	-1.60
7	+	16	NA	-	+	-	+1q, +6, +12, +13, -16q, +18	40	-6.72
8	+	32	meth	LOH	+	+	-1p36, +1q, +6q, +12, -16, -19, -22q	60	4.86
9	+	21	LOI	-	+	+	+19, +20q, -21q	50	-2.74
10	+	30	meth	NA	+	+	+1q, -2q37, +18	0	-5.98
11	+	6	meth	LOH	-	+	-1p36, -22q	0	-4.12
12	+	73	meth	LOH	NA	+	-7p, +7q, +17, -18q	0	-21.34
13	+	44	LOI	-	+	+	+1q, -7p, +7q11-q21, -7q22-q35, -11p13, -16q, -17	73	14.87
14	+	37	meth	LOH	NA	+	-11q13	0	-13.78
15	-	34	LOI	-	+	+	+1q, +12, -16q, +17, +18	75	8.98
16	+	53	LOI	-	+	+	-10p, +10q, -14q, -16	0	-10.06
17	+	46	LOI	-	+	+	+1q, -6q, -16q, +18	0	-8.62
18	+	32	LOI	-	+	+	+1q, +6	0	-3.52
19	+	88	meth	LOH	+	+	+6, +7, -18q, +22q	100	18.98
20	+	8	LOI	-	+	+	-1p36, +12, -16, +17, +18	75	6.05
21	+	36	LOI	-	+	+	-1p36, +1p35-1q43, -1q44, -2q37, -7p22, +7q21, -12q24, +18, -19	71	15.36
22	+	17	LOI	-	+	-	-1p36, +3q, +6, +8, +13, -16q, -22q	22	-11.14
23	+	22	meth	LOH	+	+	None	NA	0
24	+	24	LOI	-	+	+	-1p36, -2q37, +8, -22q	67	4.31
25	+	12	LOI	-	+	+	+1q, +12, -12q24, +18	67	5.57

system (K4006 DAKO) at a dilution of 1:150 for Ki-67/WT1 and 1:200 for IGF-II according to the manufacturer's instructions. Antigen retrieval for WT1 was carried out by pepsin digestion in 0.2 mol/L HCl at 37°C in a humidified chamber; the slides were boiled in 10 mmol/L Tris/NaOH, 1 mmol/L EDTA (pH 9) in a pressure cooker for 2 min for Ki-67 and in 10 mmol/L citric acid (pH 6) in the microwave for 9 min for IGF-II. Ki-67 proliferation index was determined by manually counting 1,000 cells per slide, of which the positively stained cells determined the percentage of proliferation. Samples with 5% to 20% positive cells were classified as actively proliferating, with cases >20% positive regarded as highly proliferative. IGF-II expression was classified as negative, weakly positive, or strongly positive relative to normal kidney.

Results

PLNRs overexpress IGF-II due to genetic and epigenetic mechanisms. We examined genetic and epigenetic alterations at the 11p15 locus in our series of PLNRs by means of LOH and methylation analysis. We identified LOH in 10 of 39 (26%) informative cases (Fig. 1A). In only one case (PLNR06) was LOH observed in the rest and not the tumor. *H19* hypermethylation by pyrosequencing was present in 37 of 40 (93%) assessable PLNRs. *IGF-II* LOI, identified by means of *H19* hypermethylation in the absence of allelic imbalance, was observed in 23 of 33 (70%) cases where data from both assays were available (Fig. 1B). We investigated IGF-II expression by quantitative reverse transcription-PCR (RT-PCR) and immunohistochemistry and observed in all but 2 cases (40 of 42, 95%) high levels of the transcript (21 of 34) and/or the protein (30 of 42; Table 1).

PLNRs can harbor large-scale changes in DNA copy number. To determine whether additional genomic events were associated with the earliest stages of IGF-driven Wilms tumorigenesis, we carried out aCGH on our series of 50 PLNRs (Table 1). The genomic profiles of PLNRs could be subdivided into three categories: those with no copy number changes; those with single, whole chromosome alterations; and those with multiple gains and losses. In 22 of 50 (44%) of our cases, there were no alterations in DNA copy number detectable by our platform. These include relatively large, hyperplastic PLNRs with WT1 protein expression (Fig. 2A). It is of note that, in an earlier aCGH study of Wilms tumors, we similarly observed 24% of cases to harbor no such copy number changes (14).

Eight of 50 (16%) PLNRs exhibited only a single chromosomal alteration. This was loss of 1p and 11p in two cases each and single examples of -11q, -12q24, -21q, and +X (Fig. 2B). The remaining rests harbored multiple chromosomal aberrations (Fig. 2C). Taken together, the most frequent aberrations included loss of 1p (7 of 50, 14%) and gain of chromosomes 18 (6 of 50, 12%), 13 (5 of 50, 10%), 10p15 (4 of 50, 8%), and 12 (3 of 50, 6%; Fig. 3). PLNRs with adenomatous features harbored more copy number changes than those without (3.3 versus 1.0; $P < 0.001$, Fisher's exact test). There were no significant differences in rests from bilateral versus unilateral patients.

There were no statistically significant associations of gross copy number changes in PLNRs with LOH versus LOI at 11p15. As allelic imbalances and copy number losses of 11q and 16q have been reported to associate with *IGF-II* LOI in Wilms tumors (19), we further analyzed LOH at these loci in our PLNRs. 11q LOH was observed in three cases (PLNR11, PLNR15, and PLNR22), all of which had LOI in our series. LOH at 16q was observed in only a single, LOI-positive rest

(PLNR22), intriguingly in a case where the concurrent Wilms tumor was of anaplastic histology.

Evidence for a nonobligate malignant progression from PLNR to Wilms tumor. For a subset of our samples (n = 25), we were able to directly compare the aCGH profiles of the PLNRs and their concurrent Wilms tumors. For the majority (19 of 25, 76%) of cases, the Wilms tumors harbored the same copy number changes as those observed in the associated rest (Table 1). In three cases, the profiles were identical (Fig. 4A); however, for the most part, the tumors contained further changes in addition to those observed in the PLNR (Fig. 4B). There were quantitatively more alterations in Wilms tumors than rests (median, 4 versus 1; $P < 0.001$, Mann-Whitney U test), even when those cases with no copy number changes were excluded (median, 4 versus 3; $P = 0.011$, Mann-Whitney U test).

To probe more rigorously the differences and similarities between PLNRs and Wilms tumors, we took several statistical approaches. Firstly, we applied class comparison techniques between our complete series of 50 PLNRs and 25 Wilms tumors (all from FFPE) and our larger published series of 76 frozen Wilms tumor specimens (14) to look for widespread differences between the lesions. A Fisher's exact test, corrected for multiple testing, revealed few statistically significant differences between rests and Wilms tumors, reflecting the common genetic alterations present between the precursor and the cancer. There were, however, two significantly different loci, gain of 1q and loss of 16q, which were present in Wilms tumors but not observed in PLNRs in our series (Fig. 4C).

In addition, we were able to apply paired statistics for our 25 patient-matched cases to reduce between-subject variability and

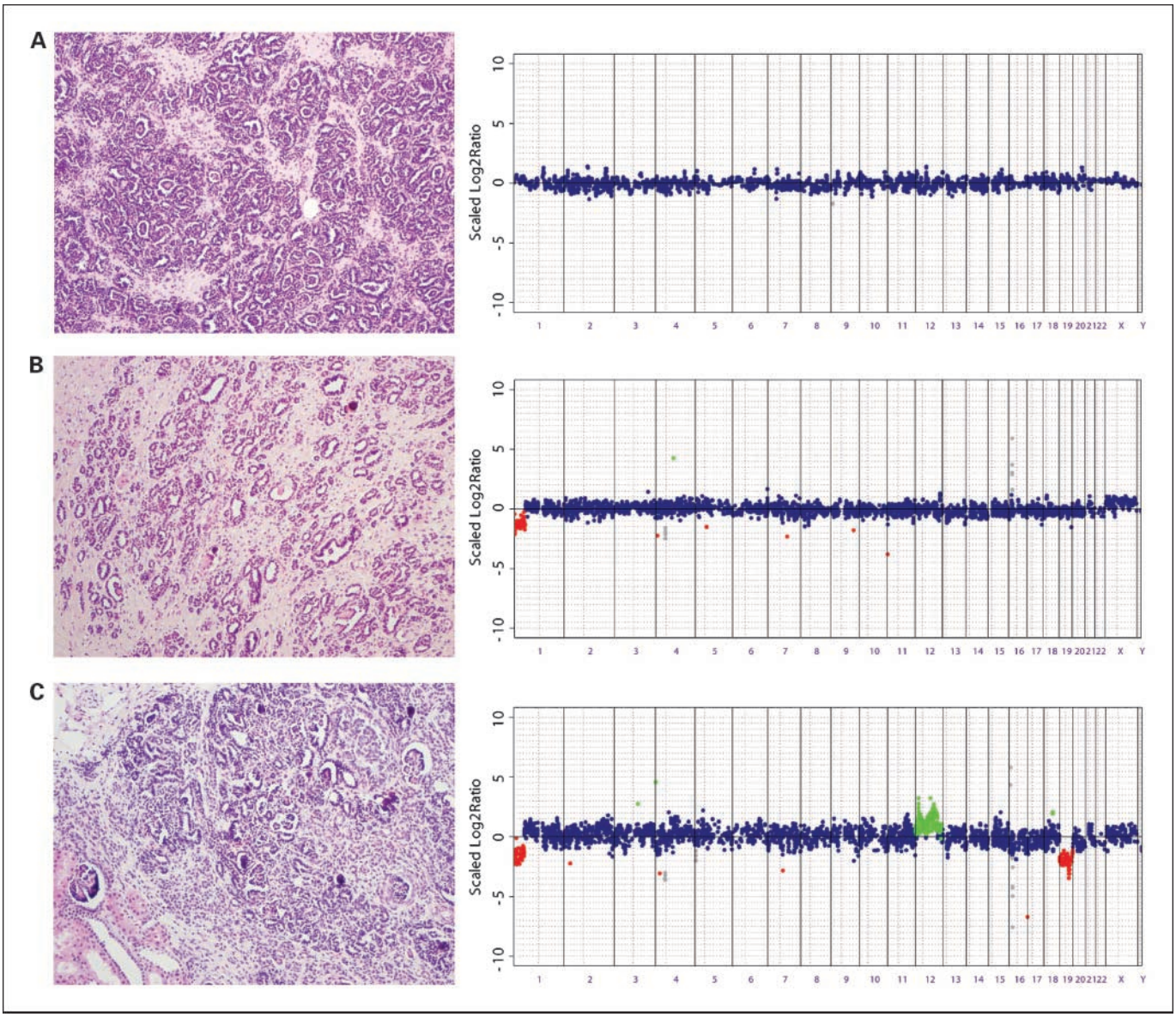

Fig. 2. Copy number changes in PLNRs. Genome plots from aCGH with $\log_2$ ratios for each clone (*Y axis*) plotted according to chromosomal location (*X axis*). *Horizontal line,* centromere. *Green,* gains; *red,* losses. *A,* sclerosing PLNR47 (H&E, ×100), showing no large-scale changes in DNA copy number. *B,* sclerosing PLNR16 (H&E, ×100), showing a single alteration, loss of 1p36. *C,* sclerosing/adenomatous PLNR08 (H&E, ×100), harboring multiple changes including loss of 1p36, gain of 12, and loss of 19.

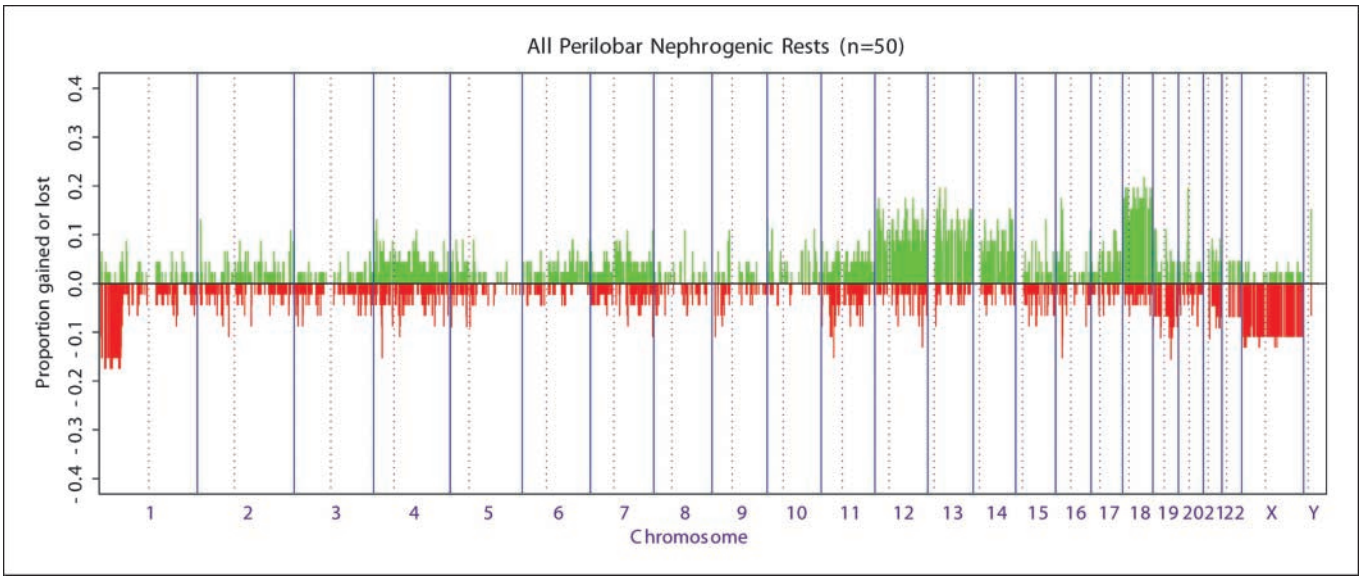

Fig. 3. Summary of copy number changes by aCGH in PLNRs. The proportion of tumors in which each clone is gained (*green bars*) or lost (*red bars*) is plotted (*Y axis*) for each BAC clone according to genomic location (*X axis*). *Vertical dotted lines,* chromosome centromeres.

to track the molecular evolution of specific tumors. Using the paired significance analysis of microarrays algorithm on our segmented data again highlighted +1q and -16q as significant alterations "acquired" in the development from PLNR to Wilms tumor. This analysis showed that gains of chromosome 6 and losses at 10p and 14q were significantly associated with the later stages of Wilms tumorigenesis, as these were also not seen in rests (Fig. 4D).

Furthermore, we calculated both concordance and similarity scores for our PLNR/Wilms tumor pairs as described by Waldman et al. (17). For the majority of rests with detectable genomic alterations (9 of 15, 60%), the similarity score between a given rest and its associated Wilms tumor was considerably higher than for the remaining tumors (Fig. 5, *blue filled circles*), and the concordance between pairs was high (>50%). In two cases, there was only a single higher score for the PLNR in the series of unmatched tumors. Cases of PLNR with no copy number changes inevitably had a low score when compared with the tumors (Fig. 5, *gray filled circles*).

Although these data are consistent with the notion that PLNRs are the molecular genetic precursor of the associated Wilms tumors, there were a few samples in which this model did not fit. In six cases, PLNRs harbored large-scale copy number changes not observed in the concurrent Wilms tumor (Table 1). These included the samples that contained the lowest similarity scores between the rest and matched tumor (Fig. 5). There were three recurrent aberrations noted in these rests: gain of 18 (commonly seen in Wilms tumor) and 10p and 14q (rarely reported in Wilms tumors). All of these PLNRs had a low proliferative index by Ki-67 immunohistochemistry. It is apparent from these data, and from five cases consisting of 13 multifocal lesions with differing genomic profiles (Table 1), that although the evidence for PLNRs as precursors is compelling, not all lesions must necessarily undergo malignant transformation.

Actively proliferating PLNRs represent a more advanced molecular genetic precursor. We investigated the genomic profiles of our entire series of PLNRs based on the proliferation index assessed by Ki-67 staining. Sixteen of 50 (32%) PLNRs were classified as actively proliferating (4 of 50, 8% were highly proliferative) in contrast with 24 of 25 (96%) Wilms tumors (14 of 25, 56% highly proliferative; Table 1). There were a greater number of copy number changes in proliferating versus nonproliferating PLNRs (median, 2 versus 0.5; $P = 0.024$, Mann-Whitney U test). In particular, the qualitative differences between these high and low proliferation index rests was such that the aCGH profiles of highly proliferating PLNRs more closely resembled their associated Wilms tumor than did those with no Ki-67 immunoreactivity [mean Spearman rank correlation coefficient, 0.583 (range, 0.489-0.641) versus 0.214 (range, 0.029-0.430); $P < 0.001$, Mann-Whitney U test]. In addition, actively proliferating PLNRs/wild-types had a significantly higher similarity score (median, 4.86 versus -6.015; $P = 0.023$, Mann-Whitney U test). Indeed, in some instances, the distinction cannot be made based on the genetic, epigenetic, or genomic data between actively proliferating, morphologically hyperplastic blastemal cells as part of a PLNR or an adjacent Wilms tumor (Fig. 4A).

Discussion

Here, we present the first genome-wide profiling of copy number changes in PLNRs and associated Wilms tumors. The proposed precursor status of both PLNRs and ILNRs has been largely defined by epidemiologic (20, 21), morphologic (3, 22, 23), but only recently by molecular (6) evidence. Here, we show clear clonal progression based on copy number profiles of PLNRs and Wilms tumors.

The route by which Wilms tumors arise from ILNRs is believed to be accompanied by mutations and deletions of *WT1* at 11p13 at an early developmental stage (5), followed by mutation and nuclear localization of β-catenin during the progression to Wilms tumor (24), with Wnt pathway activation and downstream transcription factor activation. This sequence

of events is strongly associated with a stromal histology in the subsequent Wilms tumor (11).

By contrast, PLNRs and the Wilms tumors accompanying or arising from them have been associated with dysregulation at the 11p15 locus by genetic and epigenetic means, leading to an overexpression of IGF-II (12). The molecular events accompanying this IGF-II-driven pathway have not been elucidated, although it has been suggested previously that Wilms tumors with wild-type *WT1* (presumably largely developed via the PLNR pathway) harbored more genetic alterations than those with *WT1* mutations (ILNR pathway; ref. 25).

We have determined the temporal order of changes in DNA copy number, which occur during the IGF-II/PLNR pathway of Wilms tumorigenesis. Large-scale chromosomal alterations such as gain of 12, 13, and 18, and loss of 1p were frequently observed in PLNRs and can be regarded as "early" events. This is in contrast to other common Wilms tumor-associated alterations, gain of 1q and 6 and loss of 10p and 16q, which were not observed in our PLNRs and are therefore "later" events in the proposed multistep model of Wilms tumor development.

It is of interest to note the disparity in timing between the copy number changes most convincingly associated with

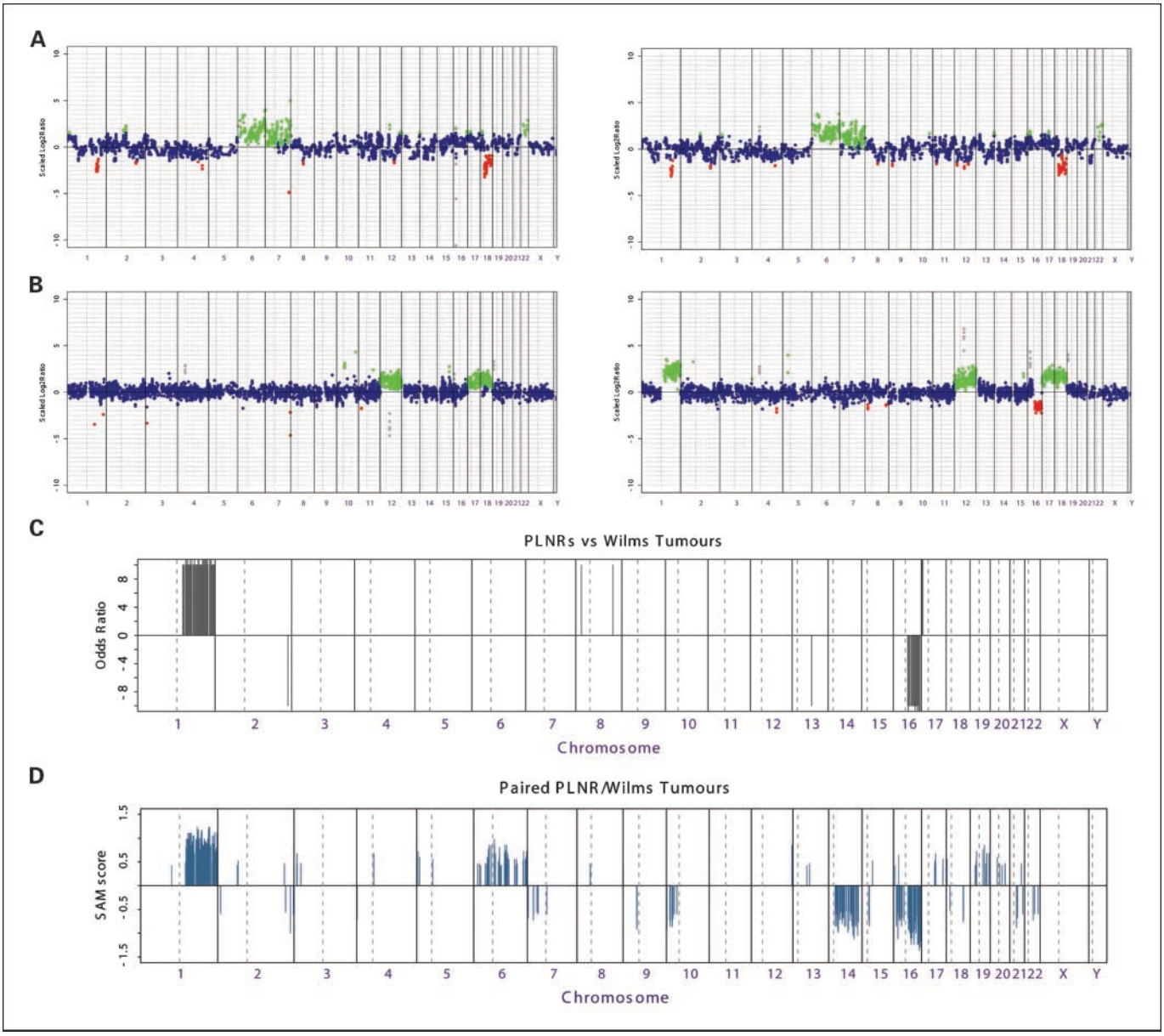

Fig. 4. Comparison of genomic profiles of PLNRs and Wilms tumors. *A,* genome plots for the hyperplastic PLNR19 and associated mixed Wilms tumor WT19 from the same patient, with identical copy number profiles: +6, +7, -18, and +22q. *B,* genome plots showing molecular evolution during Wilms tumorigenesis in a single patient, with additional copy number changes (+1q and -16q) in the blastemal/mixed Wilms tumor WT15 compared with the sclerosing PLNR15 (+12, +17, and +18). Log_2 ratios for each clone (*Y axis*) plotted according to chromosomal location (*X axis*). *Horizontal line,* centromere. *C,* categorical analysis of copy number changes between PLNRs and Wilms tumors, calculated by Fisher's exact tests on the segmented values for each clone. Those with a permutation-corrected $P < 0.05$ are plotted (odds ratio; *Y axis*) according to genomic location (*X axis*). *D,* paired significance analysis of microarrays of copy number changes between matched PLNRs and Wilms tumors. Those with a false discovery rate < 0.1 are plotted (significance analysis of microarrays score; *Y axis*) according to genomic location (*X axis*).

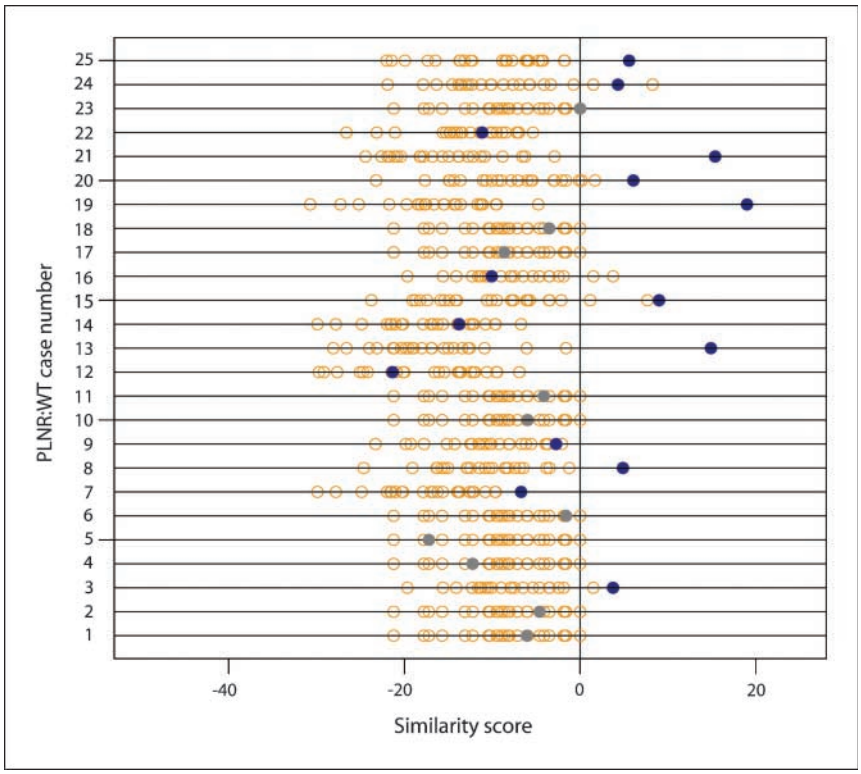

Fig. 5. Similarity scores for pairs of PLNRs and Wilms tumors. *Horizontal lines,* distribution of similarity scores for each individual PLNR and all profiled Wilms tumors based on the aCGH data (*orange circles*). *Closed circle,* appropriately matched tumor. *Gray circles,* cases where the PLNR harbored no copy number changes detected by aCGH; *blue circles,* rests with genomic alterations.

treatment failure and tumor relapse. Although loss of 1p was frequently observed in PLNRs, gain of 1q and loss of 16q were restricted to Wilms tumors. These three events have shown concordance in previous Wilms tumor profiling experiments, suggesting a common mechanism (14). The data provided here suggest a sequence in which the copy number loss of 1p occurs before a coordinated +1q/-16q at least via the IGF-II/PLNR pathway. The implication of this is that we would therefore expect the formation of an isochromosome 1q to also be associated with the WT1/ILNR pathway, although this remains to be determined.

Genetic loss at 16q has been associated previously with LOI at 11p15 (19, 26), with the gene encoding CTCF, a regulator of imprinting at the *H19/IGF-II* locus, found on 16q22. Our data add weight to the evidence (6, 27) that, despite this, 16q abnormalities are later events and preceded by genetic and epigenetic up-regulation of *IGF-II*. In the single PLNR in which we observed not a copy number change, but allelic loss, of 16q, the associated Wilms tumor was of anaplastic histology, a subtype strongly associated with mutations in *TP53* (28). We were not able to determine the timing of the event in this case. Other correlates of *IGF-II* LOI in Wilms tumors have been reported as 11q loss and trisomy 12 (19). Although we observed copy number gain of chromosome 12 and both LOH and loss at 11q in our rests, suggesting that these are early events with the IGF-II/PLNR pathway, neither correlated directly with LOI.

In around half of the PLNRs we profiled, no large-scale changes in DNA copy number were observed. This is around twice the proportion of Wilms tumors that gave similarly copy neutral aCGH profiles (14) or normal karyotypes (29). Almost all of these cases, however, exhibited high levels of IGF-II expression due to either LOI or LOH (and assumed uniparental disomy). Although this suggests that, in some cases, the genetic/epigenetic targeting of *IGF-II* is sufficient in its own right to drive the tumorigenic process through to blastemal cell persistence, which additional abnormalities may be required for tumor progression are yet to be identified. Alterations at the genetic, epigenetic, transcript, small RNA, and/or post-translational modification levels may all play a role. In any case, the observation that those rests that were actively proliferating harbored more genomic alterations, and more closely resembled their associated Wilms tumors, suggests that, in a proportion of cases at least, there are additional alterations driving clonal expansion and selection for the malignant phenotype (30).

In a small number of cases, the genomic profiles of PLNRs did not match with either the associated Wilms tumor or a topographically distinct rest. Given the often multifocal nature of PLNRs, this is perhaps not surprising, although it has not been shown before. This evidence seems to suggest that PLNRs are nonobligate precursors, in that not all lesions necessarily develop into Wilms tumors, a fact clear from the seminal early studies by Beckwith, who reported that ~1 in 100 kidneys at birth harbor nephrogenic rests, whereas the incidence of Wilms tumor is only 1 in 10,000 (3, 20). We provide a molecular underpinning of this observation in patients who did develop Wilms tumor, showing that certain lesions, often containing +10p and/or +14, may be genomic dead-ends, as their associated tumor, and Wilms tumors in general, did not harbor these alterations. It is possible that genomic gains at these loci may even actively promote regression or involution of the rest, an intriguing thought given that they are otherwise commonly lost in Wilms tumors themselves. By contrast, the frequent occurrence of +18 in these and other PLNRs and Wilms tumors suggest it to be in

some instances a noncritical mutation in sporadic IGF-II/PLNR Wilms tumorigenesis.

Although Wilms tumors have been classified as "PLNR-like" and "ILNR-like" based on their associated precursor lesion and appear to evolve by different genetic and epigenetic pathways, the two routes may incorporate significant cross-talk. The novel X-chromosome tumor suppressor gene, *WTX*, acts as a negative regulator of β-catenin in the cytoplasm, and *WTX* mutations may also drive nuclear localization of β-catenin and subsequent up-regulation of its transcriptional targets (31). Unfortunately, we have not been able to address whether *WTX* deletion occurs early in development and is thus present in the PLNRs, as our array platform does not contain a suitable BAC clone at the Xq11 locus. Additionally, WT1 itself may act as a transcriptional repressor of both *IGF-II* (32) and its receptor, *IGF-I receptor* (33), which may in turn mediate the nuclear translocation of β-catenin (34). The IGF-II/IGF-I receptor axis has recently been identified as playing a direct and central role in the self-renewal of embryonic stem cells (35). Immature blastemal cells, stem cells of the developing kidney, are more likely to predominate in the IGF-II/PLNR Wilms tumors (12) and IGF-I receptor may also be up-regulated in Wilms tumor blastema by genomic means (13). Deconvoluting the critical initiating steps and functional endpoints of these two developmental pathways is a key challenge for Wilms tumor biology.

Disclosure of Potential Conflicts of Interest

No potential conflicts of interest were disclosed.

Acknowledgments

We thank the Children's Cancer and Leukaemia Group Tumour Bank, which is funded by Cancer Research UK; the contributing pathologists, oncologists, and surgeons for access to samples; and Boo Messahel (Institute of Cancer Research), Lorna Tinworth (St George's Hospital Medical School), and Michelle Lazenby and Mandy Gilkes (Department of Haematology, Cardiff University) for technical assistance.

References

1. Schedl A. Renal abnormalities and their developmental origin. Nat Rev Genet 2007;8:791–802.
2. Rivera MN, Haber DA. Wilms tumour: connecting tumorigenesis and organ development in the kidney. Nat Rev Cancer 2005;5:699–712.
3. Beckwith JB, Kiviat NB, Bonadio JF. Nephrogenic rests, nephroblastomatosis, and the pathogenesis of Wilms tumor. Pediatr Pathol 1990;10:1–36.
4. Fukuzawa R, Reeve AE. Molecular pathology and epidemiology of nephrogenic rests and Wilms tumors. J Pediatr Hematol Oncol 2007;29:589–94.
5. Park S, Bernard A, Bove KE, et al. Inactivation of WT1 in nephrogenic rests, genetic precursors to Wilms tumour. Nat Genet 1993;5:363–7.
6. Charles AK, Brown KW, Berry PJ. Microdissecting the genetic events in nephrogenic rests and Wilms tumor development. Am J Pathol 1998;153:991–1000.
7. Rainier S, Johnson LA, Dobry CJ, Ping AJ, Grundy PE, Feinberg AP. Relaxation of imprinted genes in human cancer. Nature 1993;362:747–9.
8. Fukuzawa R, Breslow NE, Morison IM, et al. Epigenetic differences between Wilms tumours in White and East-Asian children. Lancet 2004;363:446–51.
9. Ohlsson R, Cui H, He L, et al. Mosaic allelic insulin-like growth factor 2 expression patterns reveal a link between Wilms tumorigenesis and epigenetic heterogeneity. Cancer Res 1999;59:3889–92.
10. Bjornsson HT, Brown LJ, Fallin MD, et al. Epigenetic specificity of loss of imprinting of the IGF2 gene in Wilms tumors. J Natl Cancer Inst 2007;99:1270–3.
11. Schumacher V, Schuhen S, Sonner S, et al. Two molecular subgroups of Wilms tumors with or without WT1 mutations. Clin Cancer Res 2003;9:2005–14.
12. Ravenel JD, Broman KW, Perlman EJ, et al. Loss of imprinting of insulin-like growth factor-II (IGF2) gene in distinguishing specific biologic subtypes of Wilms tumor. J Natl Cancer Inst 2001;93:1698–703.
13. Natrajan R, Reis-Filho JS, Little SE, et al. Blastemal expression of type I insulin-like growth factor receptor in Wilms tumors is driven by increased copy number and correlates with relapse. Cancer Res 2006;66:11148–55.
14. Natrajan R, Williams RD, Hing SN, et al. Array CGH profiling of favourable histology Wilms tumours reveals novel gains and losses associated with relapse. J Pathol 2006;210:49–58.
15. Little SE, Vuononvirta R, Reis-Filho JS, et al. Array CGH using whole genome amplification of fresh-frozen and formalin-fixed, paraffin-embedded tumor DNA. Genomics 2006;87:298–306.
16. Redon R, Ishikawa S, Fitch KR, et al. Global variation in copy number in the human genome. Nature 2006;444:444–54.
17. Waldman FM, DeVries S, Chew KL, Moore DH II, Kerlikowske K, Ljung BM. Chromosomal alterations in ductal carcinomas *in situ* and their *in situ* recurrences. J Natl Cancer Inst 2000;92:313–20.
18. Natrajan R, Louhelainen J, Williams S, Laye J, Knowles MA. High-resolution deletion mapping of 15q13.2-q21.1 in transitional cell carcinoma of the bladder. Cancer Res 2003;63:7657–62.
19. Watanabe N, Nakadate H, Haruta M, et al. Association of 11q loss, trisomy 12, and possible 16q loss with loss of imprinting of insulin-like growth factor-II in Wilms tumor. Genes Chromosomes Cancer 2006;45:592–601.
20. Breslow N, Olshan A, Beckwith JB, Green DM. Epidemiology of Wilms tumor. Med Pediatr Oncol 1993;21:172–81.
21. Breslow NE, Beckwith JB, Perlman EJ, Reeve AE. Age distributions, birth weights, nephrogenic rests, and heterogeneity in the pathogenesis of Wilms tumor. Pediatr Blood Cancer 2006;47:260–7.
22. Bove KE, McAdams AJ. The nephroblastomatosis complex and its relationship to Wilms tumor: a clinicopathologic treatise. Perspect Pediatr Pathol 1976;3:185–223.
23. Beckwith JB. Nephrogenic rests and the pathogenesis of Wilms tumor: developmental and clinical considerations. Am J Med Genet 1998;79:268–73.
24. Fukuzawa R, Heathcott RW, More HE, Reeve AE. Sequential WT1 and CTNNB1 mutations and alterations of β-catenin localisation in intralobar nephrogenic rests and associated Wilms tumours: two case studies. J Clin Pathol 2007;60:1013–6.
25. Ruteshouser EC, Hendrickson BW, Colella S, Krahe R, Pinto L, Huff V. Genome-wide loss of heterozygosity analysis of WT1-wild-type and WT1-mutant Wilms tumors. Genes Chromosomes Cancer 2005;43:172–80.
26. Mummert SK, Lobanenkov VA, Feinberg AP. Association of chromosome arm 16q loss with loss of imprinting of insulin-like growth factor-II in Wilms tumor. Genes Chromosomes Cancer 2005;43:155–61.
27. Yuan E, Li CM, Yamashiro DJ, et al. Genomic profiling maps loss of heterozygosity and defines the timing and stage dependence of epigenetic and genetic events in Wilms tumors. Mol Cancer Res 2005;3:493–502.
28. Bardeesy N, Falkoff D, Petruzzi MJ, et al. Anaplastic Wilms tumour, a subtype displaying poor prognosis, harbours p53 gene mutations. Nat Genet 1994;7:91–7.
29. Gow KW, Murphy JJ. Cytogenetic and histologic findings in Wilms tumor. J Pediatr Surg 2002;37:823–7.
30. Bove KE, Lewis C, Debrosse BK. Proliferation and maturation indices in nephrogenic rests and Wilms tumor; the emergence of heterogeneity from dormant nodular renal blastema. Pediatr Pathol Lab Med 1995;15:223–44.
31. Major MB, Camp ND, Berndt JD, et al. Wilms tumor suppressor WTX negatively regulates WNT/β-catenin signaling. Science 2007;316:1043–6.
32. Lee YI, Kim SJ. Transcriptional repression of human insulin-like growth factor-II P4 promoter by Wilms tumor suppressor WT1. DNA Cell Biol 1996;15:99–104.
33. Werner H, Re GG, Drummond IA, et al. Increased expression of the insulin-like growth factor I receptor gene, IGF1R, in Wilms tumor is correlated with modulation of IGF1R promoter activity by the WT1 Wilms tumor gene product. Proc Natl Acad Sci U S A 1993;90:5828–32.
34. Chen J, Wu A, Sun H, et al. Functional significance of type 1 insulin-like growth factor-mediated nuclear translocation of the insulin receptor substrate-1 and β-catenin. J Biol Chem 2005;280:29912–20.
35. Bendall SC, Stewart MH, Menendez P, et al. IGF and FGF cooperatively establish the regulatory stem cell niche of pluripotent human cells *in vitro*. Nature 2007;448:1015–21.